

Comparative transcriptomics characterized the distinct biosynthetic abilities of terpenoid and paeoniflorin biosynthesis in herbaceous peony strains

Baowei Lu¹, Qian Gao², Xuan Wang³, Yongjian Yang¹, Pengming Liu¹, Baoliang Yang¹, Tong Chen⁴, Xin-Chang Li², Qinghua Chen¹, Fengxia An^{Corresp., 1}, Jun Liu^{Corresp. 2}

¹ Bozhou University, Bozhou, Anhui, China

² National Key Facility for Crop Resources and Genetic Improvement, Institute of Crop Science, Chinese Academy of Agricultural Sciences, Beijing, China

³ Department of Biological Sciences, Xian Jiaotong-Liverpool University, Suzhou, China

⁴ National Resource Center for Chinese Materia Medica, Academy of Chinese Medical Sciences, Beijing, China

Corresponding Authors: Fengxia An, Jun Liu

Email address: An_fengxia@163.com, liujun@caas.cn

The herbaceous peony (*Paeonia lactiflora* Pall.) is a perennial flowering plant of the Paeoniaceae species that is widely cultivated for medical and ornamental uses. The monoterpene glucoside paeoniflorin and its derivatives are the active compounds of the *P. lactiflora* roots. However, the gene regulation pathways associated with monoterpene and paeoniflorin biosynthesis in *P. lactiflora* are still unclear. Here, we selected three genotypes of *P. lactiflora* with distinct morphologic features and chemical compositions that were a result of long-term reproductive isolation. We performed an RNA-sequencing experiment to profile the transcriptome changes of the shoots and roots. Using *de novo* assembly analysis, we identified 36,264 unigenes, including 521 genes responsible for encoding transcription factors. We also identified 28,925 unigenes that were preferentially expressed in different organs and/or genotypes. Pathway enrichment analysis showed that the *P. lactiflora* unigenes were significantly overrepresented in several secondary metabolite biosynthesis pathways. We identified and profiled 33 genes responsible for encoding the enzymes controlling the major catalytic reactions in the terpenoid backbone and in monoterpene biosynthesis. Our study identified the candidate genes in the terpenoid biosynthesis pathways, providing useful information for metabolic engineering of *P. lactiflora* intended for pharmaceutical uses and facilitating the development of strategies to improve marker-assist *P. lactiflora* in the future.

1 **Comparative Transcriptomics Characterized the Distinct**
2 **Biosynthetic Abilities of Terpenoid and Paeoniflorin Biosynthesis in**
3 **Herbaceous Peony Strains**

4 Baowei Lu^{1,3}, Qian Gao², Xuan Wang^{2,3}, Yongjian Yang¹, Pengming Liu¹, Baoliang Yang¹,
5 Tong Chen⁴, Xin-Chang Li², Qinghua Chen¹, Fengxia An^{1*}and Jun Liu^{2*}

6
7 ¹Bozhou University, Anhui Province, 236800, China

8 ²National Key Facility for Crop Resources and Genetic Improvement, Institute of Crop Science, Chinese
9 Academy of Agricultural Sciences, Beijing 100081, China

10 ³Department of Biological Sciences, Xian Jiaotong-Liverpool University, Suzhou 215123, China

11 ⁴National Resource Center for Chinese Materia Medica, Academy of Chinese Medical Sciences, Beijing
12 100700, China

13
14 Corresponding Author:

15 FengxiaAn (An_fengxia@163.com) or Jun Liu (liujun@caas.cn)

30

31

32 Abstract

33 The herbaceous peony (*Paeonia lactiflora* Pall.) is a perennial flowering plant of the Paeoniaceae species that is
34 widely cultivated for medical and ornamental uses. The monoterpene glucoside paeoniflorin and its derivatives are
35 the active compounds of the *P. lactiflora* roots. However, the gene regulation pathways associated with
36 monoterpene and paeoniflorin biosynthesis in *P. lactiflora* are still unclear. Here, we selected three genotypes of
37 *P. lactiflora* with distinct morphologic features and chemical compositions that were a result of long-term
38 reproductive isolation. We performed an RNA-sequencing experiment to profile the transcriptome changes of the
39 shoots and roots. Using *de novo* assembly analysis, we identified 36,264 unigenes, including 521 genes responsible
40 for encoding transcription factors. We also identified 28,925 unigenes that were preferentially expressed in different
41 organs and/or genotypes. Pathway enrichment analysis showed that the *P. lactiflora* unigenes were significantly
42 overrepresented in several secondary metabolite biosynthesis pathways. We identified and profiled 33 genes
43 responsible for encoding the enzymes controlling the major catalytic reactions in the terpenoid backbone and in
44 monoterpene biosynthesis. Our study identified the candidate genes in the terpenoid biosynthesis pathways,
45 providing useful information for metabolic engineering of *P. lactiflora* intended for pharmaceutical uses and
46 facilitating the development of strategies to improve marker-assist *P. lactiflora* in the future.

47

48

49

50

51

52

53

54

55

56

57 Introduction

58 The herbaceous peony (*Paeonialactiflora* Pall.) is a flowering plant in the family Paeoniaceae, which is
59 native to Central and eastern Asia (Zhao et al. 2018; Zhao et al. 2017). Its dried root is harvested without the
60 bark in the autumn from plants that are between 3-5 years of age; this harvested material is named Radix
61 Paeoniae Alba or Baishao and is a well-known Chinese herb, used for over 2000 years (He & Dai 2011; Zha
62 et al. 2012). A water/ethanol extract of Radix Paeoniae Alba, now known as Total Glucosides of Peony (TGP),
63 was originally used in the treatment of typhoid (Li et al. 2011). Subsequently, TGP has been widely
64 prescribed for fever, rheumatoid arthritis, hepatitis, muscle cramping and spasms, systemic lupus
65 erythematosus, and dysmenorrhea (Fan et al. 2012; He & Dai 2011; Ji et al. 2013; Mao et al. 2012; Nam et al.
66 2013).

67 Paeoniflorin (C₂₃H₂₈O₁₁, molecular weight = 480.45) is the major medicinal component in *P. lactiflora*
68 roots. In vitro and in vivo studies in animal models have confirmed that TGP, paeoniflorin,
69 benzoylpaeoniflorin, galloylpaeoniflorin and their derivatives, are medicinally active compounds with multiple
70 pharmacological effects (Fan et al. 2012; He & Dai 2011; Zhou & Wink 2018). TGP can inhibit acute and
71 subacute inflammation, an effect which is potentially mediated by the suppression of prostaglandin E₂,
72 leukotriene B₄, and nitric oxide, as well as the intracellular calcium ion concentration (He & Dai 2011; Xu et
73 al. 2016). TGP has been known to protect cells against Ca²⁺ overload and oxidative stress (Zhang et al. 2017).
74 Moreover, the components of TGP, as important immunomodulatory effectors, can regulate the proliferation
75 and apoptosis of lymphocytes and balance the production of proinflammatory cytokines in a dose-dependent
76 manner (He & Dai 2011; Hu et al. 2018). In addition, paeoniflorin and its derivatives were shown to inhibit
77 tumor growth and macrophage-mediated lung metastases (Ou et al. 2011; Wu et al. 2015).

78 Paeoniflorin is a monoterpene glucoside that is biosynthesized from geranyl-pyrophosphate (GPP). GPP
79 is produced via a conversion from the universal terpenoid precursor, Isopentenyl pyrophosphate (IPP). In
80 plants and bacteria, IPP is produced from the two terpene biosynthesis pathways, the mevalonate pathway
81 (MVA), and the 1-deoxy-d-xylulose-5-phosphate/ methyl-erythritol-4-phosphate (DXP/MEP) pathway
82 (Kanehisa et al. 2012; Ren et al. 2009; Xie et al. 2011). The MVA pathway reactions take place in the cytosol
83 and are catalyzed by enzymes including hydroxyl methylglutaryl-CoA synthase, acetyl-CoA C-

84 acetyltransferase, HMG-CoA reductase, mevalonate kinase, and phosphomevalonate kinase. The DXP/MEP
85 pathway is catalyzed in the plastids. Pyruvate and glyceraldehyde 3-phosphate are converted by 1-deoxy-D-
86 xylulose-5-phosphate synthase and 1-deoxy-D-xylulose-5-phosphate reductoisomerase to 1-deoxy-D-xylulose
87 5-phosphate and 2-C-methyl-D-erythritol 4-phosphate, respectively. The products are subsequently catalyzed
88 by 4-diphosphocytidyl-2-C-methyl-D-erythritol (CDP-ME) synthase, CDP-ME kinase, and 2-C-methyl-D-
89 erythritol2,4-cyclodiphosphate synthase to mediate the formation of 2-C-methyl-D-erythritol 2,4-
90 cyclopyrophosphate, which is then converted to (E)-4-hydroxy-3-methyl-but-2-enyl pyrophosphate (HMB-PP)
91 by HMB-PP synthase. HMB-PP is converted to IPP and dimethylallyl pyrophosphate (DMAPP) by HMB-PP
92 reductase. IPP and DMAPP are condensed by geranyl pyrophosphate synthase to produce GPP. In addition to
93 producing a monoterpene, GPP is also a precursor to sesquiterpenes and diterpenes. The conversion from GPP
94 to alpha-terpineol is critical for producing the monoterpene, which is catalyzed by (-)-alpha-terpineolsynthase
95 (EC 4.2.3.111, RLC1). Paeoniflorin can be modified by benzoic acid and gallic acid to produce
96 benzoylpaeoniflorin and galloylpaeoniflorin, respectively. Benzoic acid and gallic acid are catalyzed by 3-
97 deoxy-7-phosphoheptulonate synthase, 3-dehydroquinate synthase, and 3-
98 dehydroquinate dehydratase/shikimate dehydrogenase.

99 With a long history of domestication and selection, the *P. lactiflora* strains used for medical purposes
100 contain high levels of paeoniflorin and are nearly completely infertile due to embryo abortion in their
101 traditional planting regions, like the Bozhou area. Strains have been reproduced through the vegetative
102 propagation of shoots for hundreds of years. Thus these *P. lactiflora* accessions are reproductively isolated and
103 may serve as suitable resources in the investigation of the genetic and molecular basis of the paeoniflorin
104 biosynthesis pathways. Using sequence homology to search for the known sequences and domains, several
105 studies identified a group of genes involved in paeoniflorin biosynthesis. For example, the previous study
106 identified 24 genes, including 8 with full-length cDNA sequences and revealed transcriptional and
107 phylogenetic associations with paeoniflorin biosynthesis (Yuan et al. 2013). However, the gene alias in the
108 paeoniflorin biosynthesis pathways and their expression patterns have not been profiled in *P. lactiflora* strains
109 on a genome-wide basis.

110 High throughput sequencing technologies have revolutionized genomic and transcriptomic studies.

111 Improved algorithms are now available for *de novo* reassembly of the transcriptome of a non-model plant
112 species without a valid reference genome sequence. In this study, we assembled the transcriptome of roots and
113 shoots derived from the 3 strains of *P. lactiflora* using *de novo* assembly analysis. By aligning the assembled
114 genes with public databases, we globally annotated 34,203 unigenes in *P. lactiflora*. These genes may have
115 potential functions. For instance, our analysis identified 521 transcription factor genes. Moreover, we profiled
116 gene expression levels and identified a group of tissue-preferential and/or strain-preferential expressed genes
117 using differential expression analysis. Of these genes, we identified the candidate genes associated with the
118 nearly completed terpenoid backbone biosynthesis pathway. We verified the expression pattern of a selective
119 group of candidate genes using the qRT-PCR assay. Our study provides a valuable dataset for updating our
120 understanding of the gene regulatory network underlying paeoniflorin biosynthesis in *P. lactiflora*.

121 **Materials and Methods**

122 **Plant materials for RNA-Seq**

123 The *P. lactiflora* Pu-Bang, Xian-Tiao, and Guan-Shang strains were conserved and cultivated under
124 field conditions at Bozhou University, Bozhou, China. The shoots and roots of 3-year old plants were
125 isolated. To avoid circadian effects, we harvested all the tissues in the afternoon of the same day. The samples
126 were frozen in liquid nitrogen immediately after harvesting. The isolated samples and purified RNA were
127 stored at -80 °C.

128 **RNA extraction, library construction, and Illumina sequencing**

129 The total RNA of individual samples was extracted and purified with the RNeasy® Plant Mini Kit
130 (QIAGEN, Germany). RNA concentration was measured using a Nanodrop 2100 spectrophotometer. RNA
131 Integrity values were checked using an Agilent Bioanalyzer. The samples with a RIN score >8.5 were used for
132 library construction (Liu et al. 2014). The sequencing libraries were generated using a NEB Next Ultra RNA
133 Library Prep Kit for Illumina (New England Biosystems), following the manufacturer's recommendations.
134 Library sequencing was performed on a Hi-Seq X10 system with 150-cycle paired-end sequencing protocol
135 (Illumina).

136 **Analysis of RNA-seq datasets**

137 Transcriptome assembly was performed using Trinity (Haas et al. 2013). Fragments per kilobase of exon

138 per million fragments mapped of assembled transcripts (FPKM) were calculated and normalized using DESeq2
139 with global normalization parameters (Anders et al. 2014; Love et al. 2014; Quinn & Chang 2016; Zhang et al.
140 2014). Differential expression analysis was carried out using DESeq2 (Anders & Huber 2010). Genes with
141 normalized fold-change greater than 2, significance P-value less than 0.05, and Benjamini-Hochberg false
142 discovery rate less than 0.1 were considered to be differentially expressed genes.

143 **Transcriptome annotation and pathway analysis**

144 The sequences of the assembled unigenes were annotated by Trinotate (Haas et al. 2013). Coding
145 regions of unigenes were predicted using Transdecoder (Haas et al. 2013). BLAST v2.7.1 was performed to
146 determine the sequence homology (e-value cutoff of $1e^{-5}$) to UniProt/SwissProt, HMMR v3.1b2, EggNOG
147 v4.5.1, and metabolic pathways were analyzed using the Kyoto Encyclopedia of Genes and Genomes database
148 (Kanehisa et al. 2015).

149 **Quantitative detection of paeoniflorin**

150 We referred to the previous method in order to measure paeoniflorin in samples (Yuan et al. 2013). The
151 dried samples (0.50 g) were weighed and extracted with 50 mL of 50% aqueous methanol with ultrasonication
152 for 30 min. The extracted samples were diluted with 50 mL 50% aqueous methanol and filtered with a 0.45-
153 μm Millipore filter membrane (Millipore, MA, USA) at 25 °C. We used the Agilent 1200 LC Series (Agilent
154 Technologies, Palo Alto, CA, USA) High Performance Liquid Chromatography (HPLC) system to measure the
155 paeoniflorin abundance. The wavelength was set at 230 nm with a flow rate of 1.0 mL/min at a temperature of
156 25 °C. Standard compounds were purchased from the National Institutes for Food and Drug Control and the
157 linearity of the standard compounds was checked at seven concentration solutions.

158 **Quantitative RT-PCR**

159 A total of 1 to 2 μg RNA samples were treated by DNase I (RNeasy plant mini kit) and were reverse
160 transcribed with oligo (dT) primer and SuperScript III (Invitrogen). cDNA samples were analyzed using
161 quantitative PCR with SYBR Premix Ex Taq (Takara) and a Biorad CFX96 real-time PCR system. The
162 conserved glyceraldehyde-3-phosphate dehydrogenase (*GAPDH*) transcript sequences were used as
163 endogenous reference genes to normalize the expression levels among samples (Qi et al. 2018). The qRT-PCR
164 reactions were carried out under 60°C annealing temperature and 40 cycles of amplification. We used three
165 technical replicates to produce the average expression levels of the genes relative to that of the reference gene

166 using the $2^{-\Delta\Delta CT}$ method (Livak & Schmittgen 2001). The primers are listed in Supplemental Table 1.

167 **Accession numbers**

168 The RNA-seq datasets (accession number PRJCA001310) are available on the Genome Sequence Archive
169 database (<http://gsa.big.ac.cn/>) in the BIG Data Center (BIG.Members. 2018; Wang et al. 2017).

170 **Results**

171 **RNA-Seq and *de novo* assembly of the *P. lactiflora* transcriptome**

172 The *P. lactiflora* Pu-Bang (PB) and Xian-Tiao (XT) accessions are the most widely used herbaceous peony
173 stains for medical uses due to their high levels of paeoniflorin, which is derived mainly from their roots; whereas
174 the Guan-Shang (GS) accession contains less paeoniflorin and is usually cultivated for ornamental uses. The
175 morphological features of the 1- and 3-year old plants of the 3 strains were shown in Figure 1, respectively. We
176 determined the paeoniflorin levels of the isolated root samples using High Performance Liquid Chromatography
177 (HPLC). The results confirmed the accumulated levels of paeoniflorin in PB and XT roots compared with
178 those of GS (Supplemental Fig. 1).

179 To systematically identify genes and explore the gene expression network underlying paeoniflorin
180 biosynthesis in *P. lactiflora*, we purified the RNA samples derived from the shoots and roots of 3-year old PB,
181 XT, and GS plants, and carried out the RNA-sequencing analysis with three biological replicates using the
182 Illumina paired-end 150 bp protocol. After filtering out the low quality reads, we obtained 775.73 million
183 reads in total (Supplemental table 2). Using Trinity (Haas et al. 2013), we performed *de novo* transcriptome
184 assembly and obtained 36,264 unigenes encoding 72,910 transcripts with 986 nt contig N50 length and 42.7%
185 average GC content.

186 **Functional annotation of expressed genes in the three *P. lactiflora* accessions**

187 Due to embryo abortion and vegetative propagation, the *P. lactiflora* accessions have been undergoing
188 reproductive isolation with a long cultivation history in the Bozhou region and were thought to be genetically
189 distinct (Zhou et al. 2002). However, the genomic evidence supporting this point is still lacking. We measured
190 the expression levels of unigenes by calculating normalized Fragments Per Kilobase of exon per million
191 fragments Mapped (FPKM). The unigenes with an FPKM value higher than 1 in at least one were used to
192 perform hierarchical clustering analysis based on the Pearson correlation efficiency. We analyzed the

193 hierarchical structure of the gene expression levels on a genome-wide basis (Fig. 2A). Most of the biological
194 replicate samples belonged to the same clusters. Principal component analysis results also showed a similar
195 result confirming a high level of reproducibility of the biological replicate samples (Fig. 2B). However, the
196 tissues and strains were distributed in different cluster clades. It was noted that all the clades derived from PB
197 and XT were separated from those of GS, suggesting that the strains for medicinal uses are genetically
198 divergent from the strains used for ornamental purposes, possibly due to the selection and reproductive
199 isolation among the strains.

200 Next, we predicted the protein-coding potential for the unigenes using the Transdecoder and searched for
201 the annotation for the unigenes by aligning the assembled transcripts and predicted peptide sequences to the
202 protein sequences annotated by Swiss-Prot, TrEMBL, Pfam, and KEGG databases using Trinotate, BLASTP,
203 and BLASTX (Boutet et al. 2016; Camon et al. 2003; El-Gebali et al. 2019; Haas et al. 2013; Kanehisa et al.
204 2017). In total, we identified 34,203 unigenes containing significant matches to the annotated genes/proteins in
205 at least one database (Fig. 3B). Of them, 28,083 (82%) were reproducibly detected by at least 2 data resources.
206 The annotation information, predicted protein sequences, and FASTA-formatted sequences of these genes
207 were provided in supplemental materials that could serve as a reference annotation for future studies
208 (Supplemental table 3).

209 Transcription factors (TFs) with DNA-binding domains are the major regulators controlling the activity
210 and specificity of the gene transcription process. We predicted genes encoding TFs in our assembled unigene
211 dataset and identified 521 TF-encoding unigenes belonging to 32 TF families (Fig. 3C). Of these, AP2/ERF,
212 bHLH, FAR1, bZIP, and HB are the most abundant TF genes. The detailed information of the TF genes was
213 provided in supplemental Table 4.

214 **Identification of tissue- and/or strain- preferentially expressed unigenes**

215 Next, we searched for the differentially expressed unigenes using paired-wise comparison between
216 different samples (fold change of expression level > 2 and false discovery rate < 0.05). Our analysis identified
217 10,125 up-regulated unigenes in roots and 11,911 in shoots. We found only 332 (3%) and 886 (7%) unigenes
218 were up-regulated in the roots and shoots of the three *P. lactiflora* strains, respectively; whereas there are 1906
219 to 3737 unigenes specifically up-regulated in the roots and/or shoots of each strain (Fig. 4). This result is

220 consistent with the fact that the three strains have been undergoing genetic separation and selection during the
221 last several centuries.

222 **Identification of genes in terpenoid and paeoniflorin biosynthesis pathway**

223 To further dissect the regulation pathways of the unigenes, we analyzed the gene list enrichment using the
224 Kyoto Encyclopedia of Genes and Genomes (KEGG) datasets and KOBAS3.0 with hypergeometric testing
225 and Benjamini and Hochberg correction (Kanehisa et al. 2012; Xie et al. 2011). In total, we identified 71
226 significantly enriched KEGG pathways in *P. lactiflora* (Supplemental Table 5). The list included several
227 KEGG terms of secondary metabolite biosynthesis, such as: Terpenoid backbone biosynthesis (P -value <
228 0.0152), Glycerophospholipid metabolism (P -value < 0.0001), Inositol phosphate metabolism (P -value <
229 0.0001), Pyruvate metabolism (P -value < 0.0002), Seleno compound metabolism (P -value < 0.0298),
230 Ascorbate and aldarate metabolism (P -value < 0.0172) and Butanoate metabolism (P -value < 0.0352).
231 *P. lactiflora* are generally known to have abundant secondary metabolites (Li et al. 2016a; Liu et al. 2017; Ma
232 et al. 2016). Our transcriptome and pathway enrichment results are consistent with the metabolism profiling
233 studies.

234 The previous studies have identified 19 EST sequences in the terpenoid backbone biosynthesis pathways
235 in *P. lactiflora*, including 7 with full-length cDNA sequences (Yuan et al. 2013). However, the genes in the
236 terpenoid backbone biosynthesis pathway have not been globally profiled and the enzyme catalyzing the
237 initiation step from GPP to monoterpenoid biosynthesis has not been identified in *P. lactiflora* yet. In our
238 datasets, we identified 32 genes with full-length CDSs encoding the enzymes controlling the major catalytic
239 reactions in MVA and MEP pathways (Fig. 5). Moreover, we identified the unigene (E_H33980_c1_g4)
240 encoding (-)-alpha-terpineol synthase (EC 4.2.3.111, RLC1) that can catalyze the conversion from GPP to
241 alpha-terpineol (Kulkarni et al. 2013b), a monoterpene precursor of paeoniflorin. Our analysis identified the
242 genes encoding the enzymes that almost completely catalyzed the reactions from the glycolysis products to the
243 terpenoid backbone and monoterpenoid biosynthesis in *P. lactiflora*.

244 We analyzed the expression patterns of the aforementioned 33 unigenes (Fig 6). With the exception of
245 *AACT1*, the genes associated with the reactions of the MVP did not clearly reveal XT- and/or PB-root
246 preferential expression patterns; whereas the genes encoding ISPF in the MEP pathway and ISPH, GGR,

247 CDPMEK, IPI2, FPS1, and RLC1 associated with I-PP to monoterpene conversion reactions showed XT-
248 and/or PB-root preferential expression patterns. To confirm the expression levels determined by the RNA-seq
249 experiment, we used a quantitative Real-time PCR (qRT-PCR) assay to measure the expression levels of
250 several unigenes (Supplemental Fig. 2). These results indicated that the different biosynthetic abilities of
251 terpenoid biosynthesis among the strains may be largely contributed to by several master genes.

252 Discussion

253 The herbaceous peony has a large and complex genome. It was estimated that the genome size of the tree
254 peony, a closely related species of *P. lactiflora*, is about 12.5 Gbp. Thus, assembling the high-quality genome
255 of *P. lactiflora* remains a challenge. Recently, transcriptome studies on a large number of plant species with
256 complex genomes, such as smooth cordgrass (*Spartina alterniflora*) (Bedre et al. 2016), buckwheat (Lu et al.
257 2018), and *Caragana korshinskii* (Li et al. 2016b), have been carried out. Transcriptome assembly is
258 currently a feasible and cost-efficient technology to globally identify genes in the *P. lactiflora* genome because
259 genome information is unavailable. In our study, we identified 36,264 unigenes. Using the homolog alignment
260 analysis, we identified a large number of these assembled unigenes encoded in known regulatory
261 domains/motifs, suggesting their molecular functions. Of these, we identified 521 transcription factor genes
262 belonging to 32 families and profiled their expression patterns. Our study identified a large number of
263 previously un-annotated genes in the *P. lactiflora* genome, which could supply valuable molecular information
264 for future functional studies.

265 Plant terpenoids are widely used as traditional herbal remedies and for their aromatic qualities.
266 Terpenoids are highly abundant in several accessions of *P. lactiflora*, suggesting a high potential for terpenoid
267 biosynthesis in them. However, the terpenoid biosynthetic pathways are not yet fully understood in
268 *P. lactiflora*. Previous studies have identified the 19 EST sequences in the terpenoid backbone biosynthesis
269 pathway in *P. lactiflora* (Yuan et al. 2013). In our study, we identify 32 unigenes in the pathway and profiled
270 their expression patterns that covered most of the reactions in the terpenoid backbone biosynthesis pathway.
271 With this data, the other unidentified gene members and the complete terpenoid backbone biosynthesis
272 pathway in *P. lactiflora* strains can be deciphered in the future, using homologous cloning, phylogenetic
273 analysis, and catalytic kinetics experiments.

274 Our transcriptome profiling analysis uncovered the tissue- and/or strain-preferential expression patterns in
275 the three *P. lactiflora* strains, suggesting the genes in the terpenoid biosynthesis pathway were diversified
276 during the selection process. These results could supply valuable molecular information for future functional
277 studies in *P. lactiflora*. Geranyldiphosphate synthases and farnesyldiphosphate synthase catalyze the important
278 branch-point reactions from GPP to monoterpenes and sesquiterpenes. The catalytic activities of the two
279 enzymes are sensitive to temperature and metal ion concentration (Kulkarni et al. 2013a). Under high
280 temperature and Mg²⁺ rich condition, the monoterpene concentration was significant higher compared with
281 those of sesquiterpenes. In our experiment, we identified several unigenes encoding Geranyldiphosphate
282 synthases and farnesyldiphosphate synthase in *P. lactiflora*. Their catalytic activities could be investigated
283 under different temperature and metal ion conditions in follow-up studies.

284 It has been known that *P. lactiflora* is highly sensitive to the photoperiod and temperature changes. The
285 accessions grown in the Bozhou region have been undergoing reproductive isolation for a long period. Thus,
286 the genetic background of each individual might be fixed. In our study, we identified a large number of genes
287 in *P. lactiflora* and found gene expression patterns in the terpenoid pathway are highly diversified among
288 different accessions. With the sequences of these genes, the phylogenetic structures and population genetics
289 backgrounds of germplasm resources could be further investigated to elucidate the domestication and selection
290 process of *P. lactiflora*.

291 Conclusion

292 Using the RNA-sequencing protocol, we assembled the exon structures of 36,264 genes in the shoots and roots
293 of three 3-year-old *P. lactiflorais* accessions, including 28,925 differentially expressed genes. We
294 systematically annotated their molecular functions by aligning their sequences with those from multiple data
295 resources. 521 transcription factor genes were identified. We identified 32 genes with full-length CDSs
296 encoding the enzymes controlling the major catalytic reactions in MVA and MEP pathways and one gene
297 encoding (-)-alpha-terpineol synthase. These genes contributed nearly complete terpenoid backbone
298 biosynthesis pathways. By profiling gene expression patterns associated with MVP, MEP pathways, and I-PP
299 to monoterpene conversation reactions, we uncovered several unigenes that were highly expressed in the roots
300 of high-paeoniflorin accessions, indicating that the different biosynthetic abilities of terpenoid biosynthesis

301 among the accessions may be largely contributed to by several master genes.

302 Author Contributions

303 F. A., B. L., and J. L. designed the experiment. B. L., Y. Y., P. L., Q. C., Y. Z. and B. Y. sampled the
304 biological materials and extracted the RNA and sequenced the libraries. T. C., F. A., J.L. and Y. W. analyzed
305 the datasets. B.L. J.L. and Y.W. prepared the figures and wrote the manuscript. All authors reviewed and
306 approved the final version of the manuscript.

307

308

309 REFERENCE

- 310 Anders S, and Huber W. 2010. Differential expression analysis for sequence count data. *Genome biology* 11:R106.
311 10.1186/gb-2010-11-10-r106
- 312 Anders S, Pyl PT, and Huber W. 2014. HTSeq—a Python framework to work with high-throughput sequencing data.
313 *Bioinformatics*:btu638.
- 314 Bedre R, Mangu VR, Srivastava S, Sanchez LE, and Baisakh N. 2016. Transcriptome analysis of smooth cordgrass
315 (*Spartina alterniflora* Loisel), a monocot halophyte, reveals candidate genes involved in its adaptation to
316 salinity. *BMC genomics* 17:657-657. 10.1186/s12864-016-3017-3
- 317 BIG.Members. 2018. Database Resources of the BIG Data Center in 2018. *Nucleic acids research* 46:D14-D20.
318 10.1093/nar/gkx897
- 319 Boutet E, Lieberherr D, Tognolli M, Schneider M, Bansal P, Bridge AJ, Poux S, Bougueleret L, and Xenarios I. 2016.
320 UniProtKB/Swiss-Prot, the Manually Annotated Section of the UniProt KnowledgeBase: How to Use the
321 Entry View. In: Edwards D, ed. *Plant Bioinformatics: Methods and Protocols*. New York, NY: Springer New
322 York, 23-54.
- 323 Camon E, Barrell D, Brooksbank C, Magrane M, and Apweiler R. 2003. The Gene Ontology Annotation (GOA)
324 Project--Application of GO in SWISS-PROT, TrEMBL and InterPro. *Comparative and functional genomics*
325 4:71-74. 10.1002/cfg.235
- 326 El-Gebali S, Mistry J, Bateman A, Eddy SR, Luciani A, Potter SC, Qureshi M, Richardson LJ, Salazar GA, Smart A,
327 Sonnhammer ELL, Hirsh L, Paladin L, Piovesan D, Tosatto SCE, and Finn RD. 2019. The Pfam protein
328 families database in 2019. *Nucleic Acids Research* 47:D427-D432. 10.1093/nar/gky995
- 329 Fan YF, Xie Y, Liu L, Ho HM, Wong YF, Liu ZQ, and Zhou H. 2012. Paeoniflorin reduced acute toxicity of aconitine in
330 rats is associated with the pharmacokinetic alteration of aconitine. *Journal of ethnopharmacology*
331 141:701-708. 10.1016/j.jep.2011.09.005
- 332 Haas BJ, Papanicolaou A, Yassour M, Grabherr M, Blood PD, Bowden J, Couger MB, Eccles D, Li B, Lieber M,
333 MacManes MD, Ott M, Orvis J, Pochet N, Strozzi F, Weeks N, Westerman R, William T, Dewey CN,
334 Henschel R, LeDuc RD, Friedman N, and Regev A. 2013. De novo transcript sequence reconstruction from
335 RNA-seq using the Trinity platform for reference generation and analysis. *Nature protocols* 8:1494-1512.
336 10.1038/nprot.2013.084
- 337 He DY, and Dai SM. 2011. Anti-inflammatory and immunomodulatory effects of paeonia lactiflora pall., a
338 traditional chinese herbal medicine. *Frontiers in pharmacology* 2:10. 10.3389/fphar.2011.00010

- 339 Hu B, Xu G, Zhang X, Xu L, Zhou H, Ma Z, Shen X, Zhu J, and Shen R. 2018. Paeoniflorin Attenuates Inflammatory
340 Pain by Inhibiting Microglial Activation and Akt-NF-kappaB Signaling in the Central Nervous System.
341 *Cellular physiology and biochemistry : international journal of experimental cellular physiology,*
342 *biochemistry, and pharmacology* 47:842-850. 10.1159/000490076
- 343 Ji Y, Wang T, Wei ZF, Lu GX, Jiang SD, Xia YF, and Dai Y. 2013. Paeoniflorin, the main active constituent of Paeonia
344 lactiflora roots, attenuates bleomycin-induced pulmonary fibrosis in mice by suppressing the synthesis of
345 type I collagen. *Journal of ethnopharmacology* 149:825-832. 10.1016/j.jep.2013.08.017
- 346 Kanehisa M, Furumichi M, Tanabe M, Sato Y, and Morishima K. 2017. KEGG: new perspectives on genomes,
347 pathways, diseases and drugs. *Nucleic Acids Research* 45:D353-D361. 10.1093/nar/gkw1092
- 348 Kanehisa M, Goto S, Sato Y, Furumichi M, and Tanabe M. 2012. KEGG for integration and interpretation of large-
349 scale molecular data sets. *Nucleic acids research* 40:D109-114. 10.1093/nar/gkr988
- 350 Kanehisa M, Sato Y, Kawashima M, Furumichi M, and Tanabe M. 2015. KEGG as a reference resource for gene and
351 protein annotation. *Nucleic acids research* 44:D457-D462.
- 352 Kulkarni R, Pandit S, Chidley H, Nagel R, Schmidt A, Gershenzon J, Pujari K, Giri A, and Gupta V. 2013a.
353 Characterization of three novel isoprenyl diphosphate synthases from the terpenoid rich mango fruit.
354 *Plant physiology and biochemistry : PPB* 71:121-131. 10.1016/j.plaphy.2013.07.006
- 355 Kulkarni R, Pandit S, Chidley H, Nagel R, Schmidt A, Gershenzon J, Pujari K, Giri A, and Gupta V. 2013b.
356 Characterization of three novel isoprenyl diphosphate synthases from the terpenoid rich mango fruit.
357 *Plant Physiology and Biochemistry* 71:121-131. <https://doi.org/10.1016/j.plaphy.2013.07.006>
- 358 Li B, Bhandari DR, Rompp A, and Spengler B. 2016a. High-resolution MALDI mass spectrometry imaging of
359 gallotannins and monoterpene glucosides in the root of Paeonia lactiflora. *Scientific reports* 6:36074.
360 10.1038/srep36074
- 361 Li J, Chen CX, and Shen YH. 2011. Effects of total glucosides from paeony (Paeonia lactiflora Pall) roots on
362 experimental atherosclerosis in rats. *Journal of ethnopharmacology* 135:469-475.
363 10.1016/j.jep.2011.03.045
- 364 Li S, Fan C, Li Y, Zhang J, Sun J, Chen Y, Tian C, Su X, Lu M, Liang C, and Hu Z. 2016b. Effects of drought and salt-
365 stresses on gene expression in Caragana korshinskii seedlings revealed by RNA-seq. *BMC genomics*
366 17:200-200. 10.1186/s12864-016-2562-0
- 367 Liu D, Wang D, Qin Z, Zhang D, Yin L, Wu L, Colasanti J, Li A, and Mao L. 2014. The SEPALLATA MADS - box protein
368 SLMBP21 forms protein complexes with JOINTLESS and MACROCALYX as a transcription activator for
369 development of the tomato flower abscission zone. *The Plant Journal* 77:284-296.
- 370 Liu P, Xu Y, Yan H, Chen J, Shang E-X, Qian D-W, Jiang S, and Duan J-A. 2017. Characterization of molecular
371 signature of the roots of Paeonia lactiflora during growth. *Chinese Journal of Natural Medicines* 15:785-
372 793. [https://doi.org/10.1016/S1875-5364\(17\)30110-3](https://doi.org/10.1016/S1875-5364(17)30110-3)
- 373 Livak KJ, and Schmittgen TD. 2001. Analysis of relative gene expression data using real-time quantitative PCR and
374 the 2- $\Delta\Delta$ CT method. *methods* 25:402-408.
- 375 Love MI, Huber W, and Anders S. 2014. Moderated estimation of fold change and dispersion for RNA-seq data with
376 DESeq2. *Genome biology* 15:550.
- 377 Lu Q-H, Wang Y-Q, Song J-N, and Yang H-B. 2018. Transcriptomic identification of salt-related genes and de novo
378 assembly in common buckwheat (F. esculentum). *Plant Physiology and Biochemistry* 127:299-309.
379 <https://doi.org/10.1016/j.plaphy.2018.02.001>

- 380 Ma X, Chi YH, Niu M, Zhu Y, Zhao YL, Chen Z, Wang JB, Zhang CE, Li JY, Wang LF, Gong M, Wei SZ, Chen C, Zhang L,
381 Wu MQ, and Xiao XH. 2016. Metabolomics Coupled with Multivariate Data and Pathway Analysis on
382 Potential Biomarkers in Cholestasis and Intervention Effect of *Paeonia lactiflora* Pall. *Frontiers in*
383 *pharmacology* 7:14. 10.3389/fphar.2016.00014
- 384 Mao QQ, Ip SP, Xian YF, Hu Z, and Che CT. 2012. Anti-depressant-like effect of peony: a mini-review.
385 *Pharmaceutical biology* 50:72-77. 10.3109/13880209.2011.602696
- 386 Nam KN, Yae CG, Hong JW, Cho DH, Lee JH, and Lee EH. 2013. Paeoniflorin, a monoterpene glycoside, attenuates
387 lipopolysaccharide-induced neuronal injury and brain microglial inflammatory response. *Biotechnology*
388 *letters* 35:1183-1189. 10.1007/s10529-013-1192-8
- 389 Ou TT, Wu CH, Hsu JD, Chyau CC, Lee HJ, and Wang CJ. 2011. *Paeonia lactiflora* Pall inhibits bladder cancer growth
390 involving phosphorylation of Chk2 in vitro and in vivo. *Journal of ethnopharmacology* 135:162-172.
391 10.1016/j.jep.2011.03.011
- 392 Qi Z, Zhang Z, Wang Z, Yu J, Qin H, Mao X, Jiang H, Xin D, Yin Z, Zhu R, Liu C, Yu W, Hu Z, Wu X, Liu J, and Chen Q.
393 2018. Meta-analysis and transcriptome profiling reveal hub genes for soybean seed storage composition
394 during seed development. *Plant, cell & environment*. 10.1111/pce.13175
- 395 Quinn JJ, and Chang HY. 2016. Unique features of long non-coding RNA biogenesis and function. *Nat Rev Genet*
396 17:47-62. 10.1038/nrg.2015.10
- 397 Ren ML, Zhang X, Ding R, Dai Y, Tu FJ, Cheng YY, and Yao XS. 2009. Two new monoterpene glucosides from *Paeonia*
398 *lactiflora* Pall. *Journal of Asian natural products research* 11:670-674. 10.1080/10286020902980087
- 399 Wang Y, Song F, Zhu J, Zhang S, Yang Y, Chen T, Tang B, Dong L, Ding N, Zhang Q, Bai Z, Dong X, Chen H, Sun M, Zhai
400 S, Sun Y, Yu L, Lan L, Xiao J, Fang X, Lei H, Zhang Z, and Zhao W. 2017. GSA: Genome Sequence
401 Archive<sup/>. *Genomics, proteomics & bioinformatics* 15:14-18. 10.1016/j.gpb.2017.01.001
- 402 Wu Q, Chen GL, Li YJ, Chen Y, and Lin FZ. 2015. Paeoniflorin inhibits macrophage-mediated lung cancer metastasis.
403 *Chinese journal of natural medicines* 13:925-932. 10.1016/S1875-5364(15)30098-4
- 404 Xie C, Mao X, Huang J, Ding Y, Wu J, Dong S, Kong L, Gao G, Li CY, and Wei L. 2011. KOBAS 2.0: a web server for
405 annotation and identification of enriched pathways and diseases. *Nucleic acids research* 39:W316-322.
406 10.1093/nar/gkr483
- 407 Xu W, Zhao Y, Qin Y, Ge B, Gong W, Wu Y, Li X, Xu P, and Xue M. 2016. Enhancement of Exposure and Reduction of
408 Elimination for Paeoniflorin or Albiflorin via Co-Administration with Total Peony Glucosides and Hypoxic
409 Pharmacokinetics Comparison. *Molecules* 21. 10.3390/molecules21070874
- 410 Yuan Y, Yu J, Jiang C, Li M, Lin S, Wang X, and Huang L. 2013. Functional diversity of genes for the biosynthesis of
411 paeoniflorin and its derivatives in *Paeonia*. *International Journal of Molecular Sciences* 14:18502-18519.
412 10.3390/ijms140918502
- 413 Zha LP, Cheng ME, and Peng HS. 2012. Identification of ages and determination of paeoniflorin in roots of *Paeonia*
414 *lactiflora* Pall. From four producing areas based on growth rings. *Microscopy research and technique*
415 75:1191-1196. 10.1002/jemt.22048
- 416 Zhang Y, Qiao L, Xu W, Wang X, Li H, Chu K, and Lin Y. 2017. Paeoniflorin Attenuates Cerebral Ischemia-Induced
417 Injury by Regulating Ca(2+)/CaMKII/CREB Signaling Pathway. *Molecules* 22. 10.3390/molecules22030359
- 418 Zhang YC, Liao JY, Li ZY, Yu Y, Zhang JP, Li QF, Qu LH, Shu WS, and Chen YQ. 2014. Genome-wide screening and
419 functional analysis identify a large number of long noncoding RNAs involved in the sexual reproduction of
420 rice. *Genome Biol* 15:512. 10.1186/s13059-014-0512-1

- 421 Zhao D, Wang R, Liu D, Wu Y, Sun J, and Tao J. 2018. Melatonin and Expression of Tryptophan Decarboxylase Gene
422 (TDC) in Herbaceous Peony (*Paeonia lactiflora* Pall.) Flowers. *Molecules* 23. 10.3390/molecules23051164
- 423 Zhao D, Wei M, Shi M, Hao Z, and Tao J. 2017. Identification and comparative profiling of miRNAs in herbaceous
424 peony (*Paeonia lactiflora* Pall.) with red/yellow bicoloured flowers. *Scientific reports* 7:44926.
425 10.1038/srep44926
- 426 Zhou H, Hu S, Guo B, Feng X, Yan Y, and Li JJYxbApS. 2002. A study on genetic variation between wild and
427 cultivated populations of *Paeonia lactiflora* Pall. 37:383-388.
- 428 Zhou JX, and Wink M. 2018. Reversal of Multidrug Resistance in Human Colon Cancer and Human Leukemia Cells
429 by Three Plant Extracts and Their Major Secondary Metabolites. *Medicines* 5. 10.3390/medicines5040123
430
- 431
- 432

Figure 1

The developmental features of the 3 *P.lactifloras* strains

(A) shows the 30-day-old plants of XT, PB, and GS strains, which were grown from the shoots (B) isolated from 3-year-old plants. (C) and (D) show the leaves and roots of 3 year-old plants.

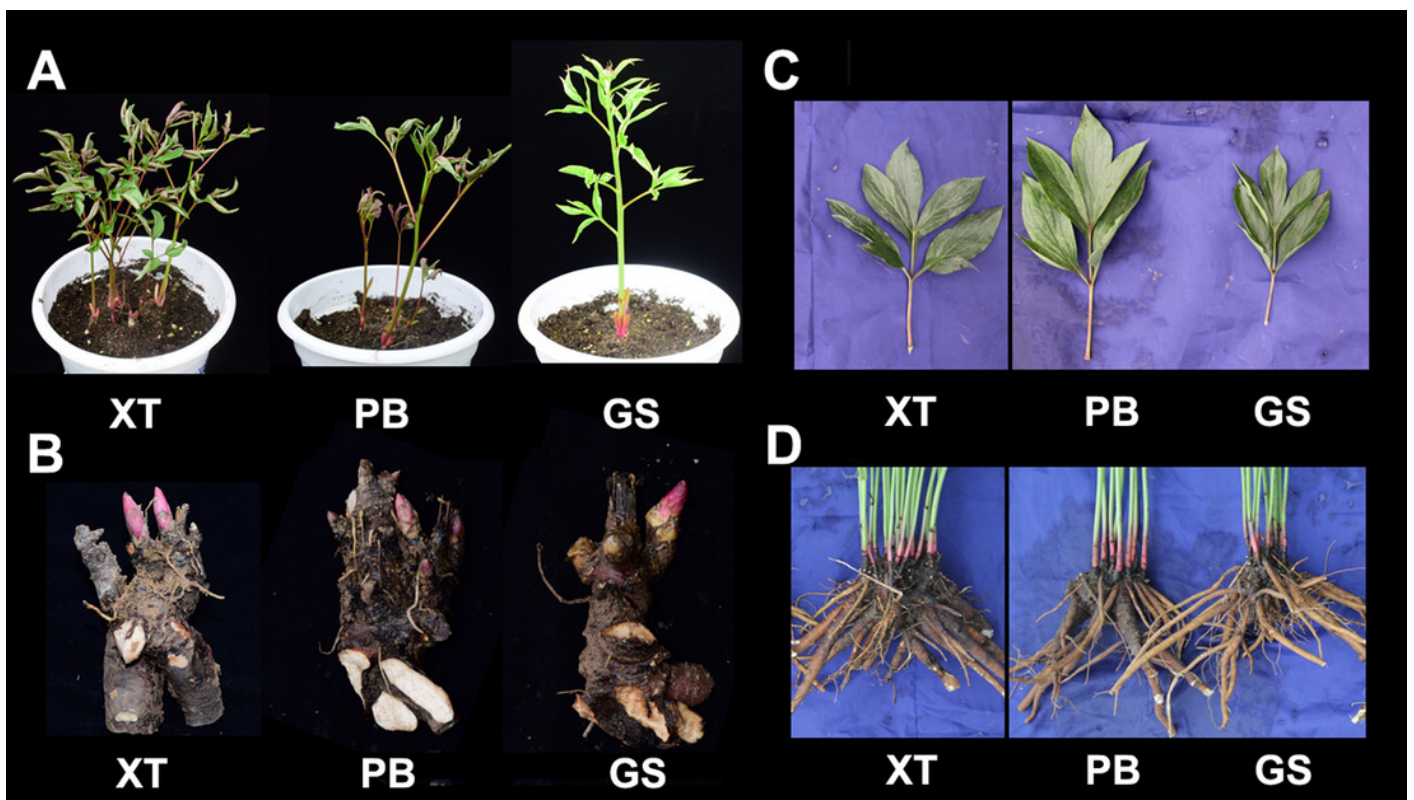


Figure 2

Figure 2. Hierarchical structure of data-sets

(A) The hierarchical structure of the gene expression levels. Genes with the FPKM values more than 1 were used for the analysis. (B) Principal component analysis for the genes.

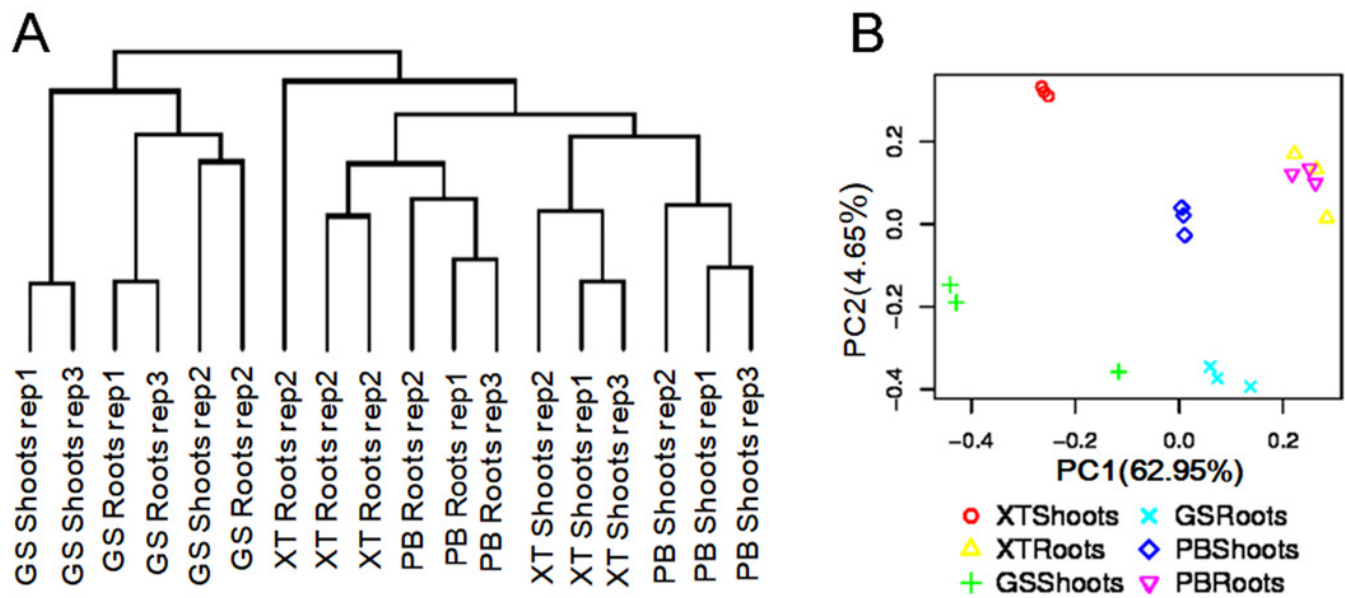


Figure 3

Figure 3. Functional annotation of unigenes

(A) The length distribution of the assembled unigenes. (B) Functional annotation of unigenes using the 4 databases. (C) Transcription factor genes identified in *P. lactiflora*.

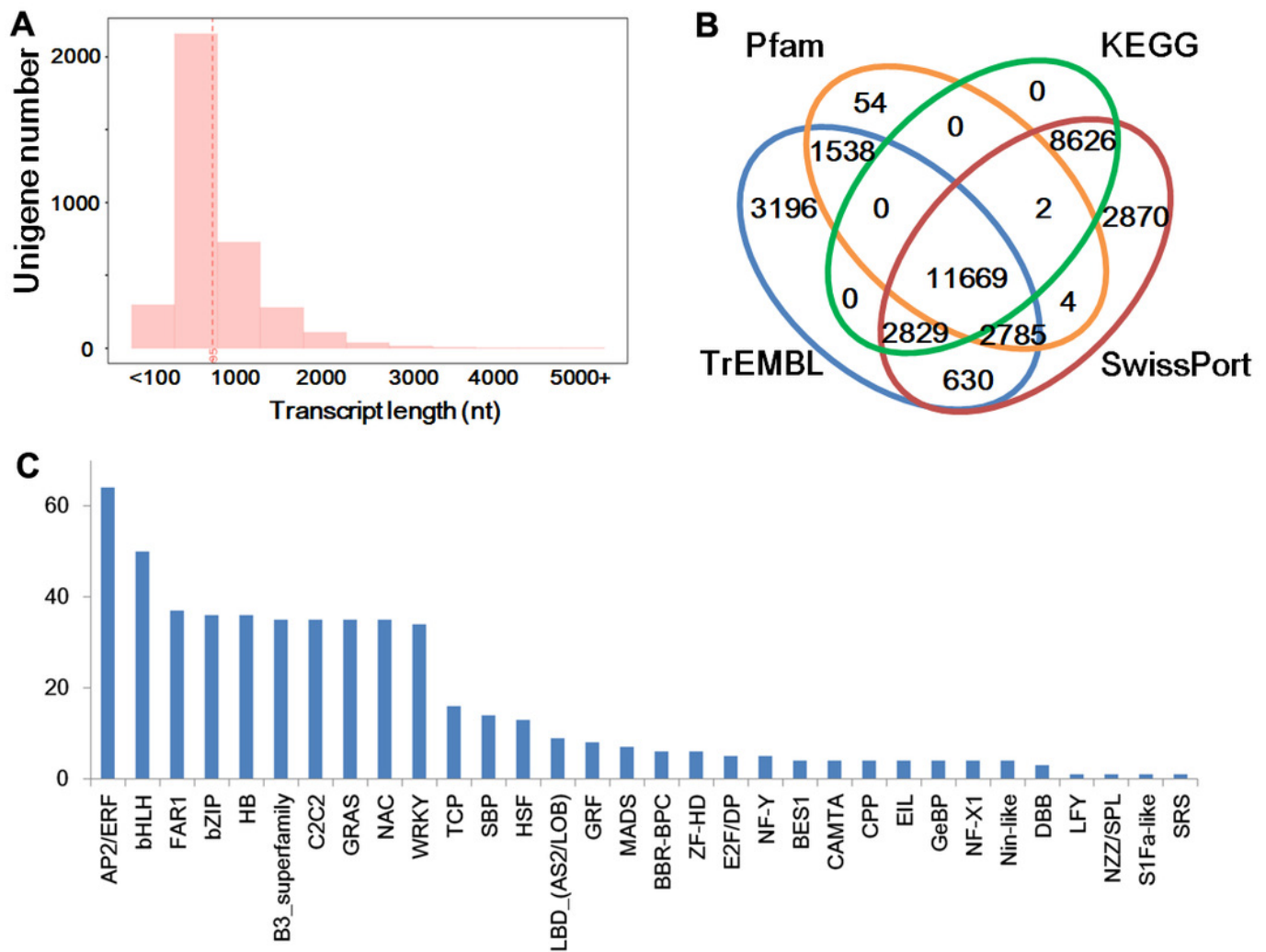


Figure 4

Figure 4. differential expression analysis of unigenes

The differentially expressed genes in roots and shoots of the three *P. lactiflora* accessions are given.

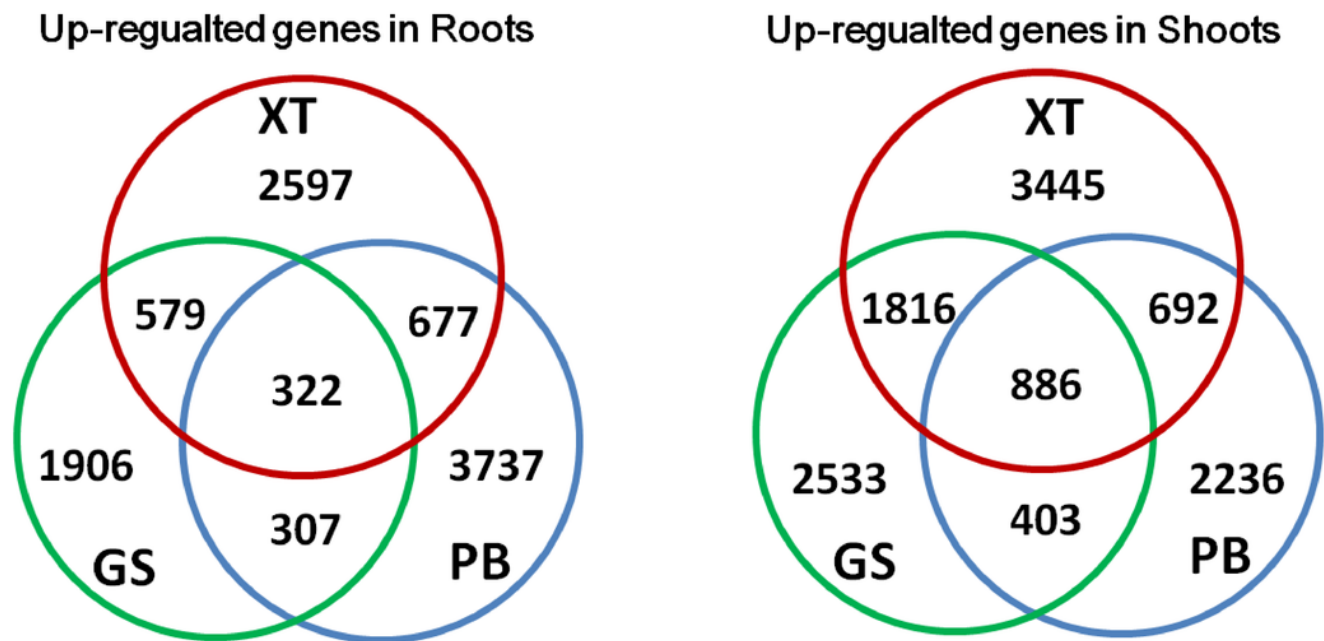


Figure 5

Figure 5. The assembled genes encoding enzymes in terpenoid backbone and monoterpene biosynthesis pathways

The identified *P. lactiflora* enzymes are highlighted by red rectangles.

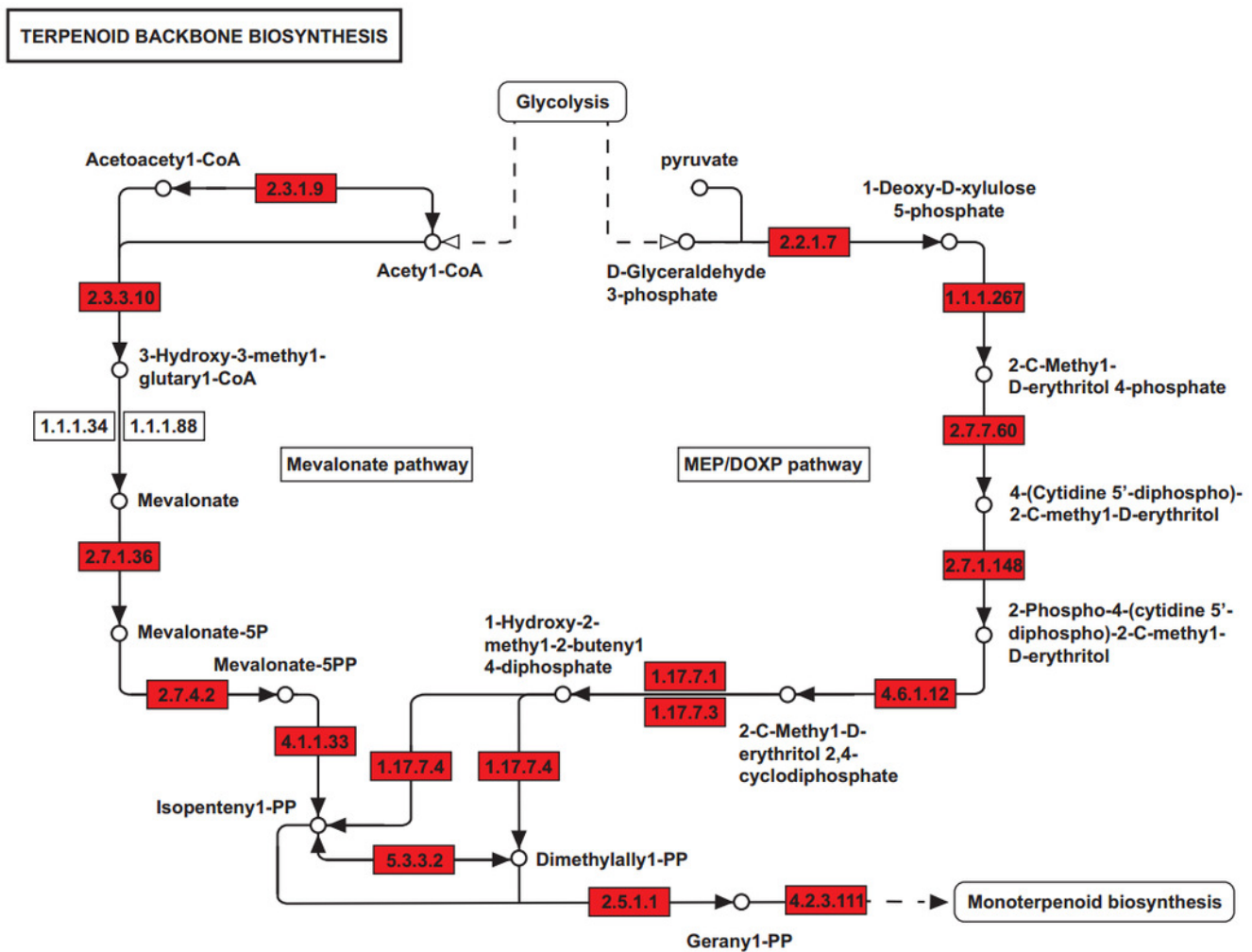


Figure 6

Figure 6. The expression levels of the genes encoding enzymes in terpenoid backbone and monoterpene biosynthesis pathways in shoot and root samples of the three *P. lactiflora* accessions.

The heatmap plot presents the mean value of expression levels of the three biological replicates. The unigene ID, enzyme id and symbols are given according to their expression levels. S and R give shoots and roots respectively.

